Supporting Text

Supporting Methods

Angeli's salt (AS) and the diethylamine/nitric oxide adduct (DEA/NO) were synthesized and used as described (1, 2). Stock solutions (>10 mM) were prepared in 10 mM NaOH and stored at –20°C. The concentrations were determined directly prior to use from the absorbance values at 250 nm (ε = 8,000 $M^{-1} \cdot cm^{-1}$; ref. 3). Unless otherwise noted, chemicals were purchased from Sigma-Aldrich and were used without further purification. The assay buffer contained the metal chelator diethylenetriaminepentaacetic acid (DTPA, 50 μM) in calcium and magnesium-free Dulbecco's PBS (pH 7.4; GIBCO/BRL). All reactions were performed at 37°C. Data reported in text and tables are mean values, and figures are representative data sets, each from $n \geq 2$ individual experiments. The SEM in Fig. 2 were of similar or smaller size than the symbol, and therefore error bars were omitted for clarity.

Plasma Analysis. The protocol was performed by using adult male mongrel dogs (22–25 kg) and was approved by the Animal Care and Use Committee of The Johns Hopkins University. Details of the surgical preparation and protocol have been reported (4, 5). Blood was withdrawn from arterial, venous, and coronary sinus catheters after 10 min of drug infusion and was centrifuged at 1,600 × *g* for 20 min at 4°C. Plasma was separated and stored at –20°C. For analysis, 0.5 ml of plasma was mixed with 0.8 ml of ethanol and centrifuged at 1,600 × *g* for 20 min. The supernatant was removed and air dried overnight at room temperature. Samples were reconstituted with assay buffer according to the manufacturer's instructions (Peninsula Laboratories) and assayed for CGRP by radioimmunoassay by using CGRP antiserum (RAS 6012). The dynamic assay range was 1–128 pg/300 μl (6). Plasma samples were also analyzed for cGMP levels with an enzyme immunoassay (Biotrak; Amersham Pharmacia) based on lyophilized samples. This assay has a detection sensitivity of 40 pM (2 fmol per well).

Heme Protein Assays. Oxidation by AS of the ferric heme proteins ferricytochrome *c* (ferricyt *c*; horse heart), ferric myoglobin (metMb; horse heart), and horseradish peroxidase (HRP) was performed in deaerated assay buffer. The buffer was first deaerated in bulk by bubbling with argon (>1 min/ml). Aliquots (3 ml) were removed by Hamilton syringe and transferred to an argon-flushed graded seal quartz cuvette (Spectrocell, Oreland, PA) stoppered with a Suba-Seal septum (Sigma-Aldrich). The buffer within the cuvette was again gently bubbled with argon for 5 min. The spectrophotometer was blanked with this solution, and an aliquot of heme protein (>1 mM stock) was added by syringe, as were aliquots of scavenger solutions (≈100 times) as appropriate. After 5 min in the instrument heat block at 37°C, AS (generally <10 μl) was added. The AS concentration was chosen to obtain reasonable absorbance changes at 550 nm within the constraints of the usable concentration range of heme protein. The rate of oxidation was monitored at 550 nm for ferricyt *c*, 575 nm for metMb, and 426 nm for HRP. The change in absorbance was determined from the amplitude of the exponential fit for each data set ($n \geq 2$ for each condition per experiment). The concentrations of AS and protein stock solutions were essentially unchanged over the course of the experiment: ferricyt *c*, 528 nm ($\varepsilon = 11 \times 10^3\ M^{-1}\cdot cm^{-1}$); metMb, 408 ($188 \times 10^3\ M^{-1}\cdot cm^{-1}$), or 502 nm ($10.2 \times 10^3\ M^{-1}\cdot cm^{-1}$) (7); HRP, 402 nm ($\varepsilon = 95 \times 10^3\ M^{-1}\cdot cm^{-1}$) (8).

Experimentally, the reaction of oxymyoglobin (oxyMb) with AS is advantageous due to the stability of the product (metMB) to air, and the experiments can be performed in triplicate in test tubes. MetMb was reduced to oxyMb [542 ($13.9 \times 10^3\ M^{-1}\cdot cm^{-1}$)] and 580 nm ($14.4 \times 10^3\ M^{-1}\cdot cm^{-1}$, ref. 7) with excess dithionite, which was removed by passage through a Sephadex G-25 M column (PD-10; Pharmacia Biotech). Typically, 25 μl of 1.6 mM oxyMb was added to 1 ml of assay buffer. Addition of 10 μl of 100× scavenger solution (2–2,000 μM final), or 10 μl of assay buffer for controls, did not significantly alter the solution pH. After addition of 10 μl of 2 mM AS, or 10 μl of 10 mM NaOH for controls, each solution was vortexed and placed in a 37°C warm room for 1 h. The data were compared as ΔAbs at 426 or 582 nm for paired triplicate sets with and without AS.

Supporting Results

Increasing concentrations of CuZnSOD (1-100 μM) reduced the yield of ferrocyt *c* (data not shown). Interestingly, the reaction of ferricyt *c* with nitrosyl hydride (HNO) in the presence of CuZnSOD appeared to be catalytic such that ferrocyt *c* formation plateaued at approximately one-third the value obtained in the absence of CuZnSOD. As previously reported (9), several reactions may occur in this system

$$Fe(III) + HNO \rightarrow Fe(II) + NO + H^+ \qquad [\mathbf{a}]$$

$$Cu(II) + HNO \rightarrow Cu(I) + NO + H^+ \qquad [\mathbf{b}]$$

$$HNO + NO \rightarrow N_2O_2^- + H^+ \qquad [\mathbf{c}]$$

The product of Eq. **c**, $N_2O_2^-$, can subsequently react with Cu(I) formed from scavenging of HNO by SOD (Eq. **b**) to regenerate Cu(II), thus providing a catalytic mechanism

$$Cu(I) + N_2O_2^- + H^+ \rightarrow Cu(II) + N_2O + H_2O \qquad [\mathbf{d}]$$

Quenching of ferrocyt *c* formation plateaus at approximately one-third the value obtained in the absence of CuZnSOD. This may be due to further reaction of $N_2O_2^-$ with NO to form $N_3O_3^-$

$$N_2O_2^- + NO \rightarrow N_3O_3^- \qquad [\mathbf{e}]$$

which in turn may reduce ferricyt *c* more efficiently than CuZnSOD

$$Fe(III) + N_3O_3^- \rightarrow Fe(II) + 3NO \qquad [\mathbf{f}]$$

Kinetic Evaluation

Table 2 provides a comparison of the affinity of HNO for different biomolecules. From these data, the relative reactivity toward HNO is oxyMb > GSH, HRP > NAC, CuZnSOD, MnSOD, metMb ~ catalase > Tempol, ferricyt *c* > O_2 (GSH, reduced glutathione; NAC, *N*-acetylcysteine). To quantify the rate constants, a known value is required. Dimerization of HNO has been estimated to have a rate constant of 4×10^9 $M^{-1} \cdot s^{-1}$ (10), based on a pK_a of 4.7 (11). Recently, however, Shafirovich and Lymar (12) reported a revised rate constant of 8×10^6 $M^{-1} \cdot s^{-1}$ by using flash photolysis techniques. If we assume that the data in Fig. 1 are a function only of competition between reduction of ferricyt *c* and dimerization (Scheme 2),

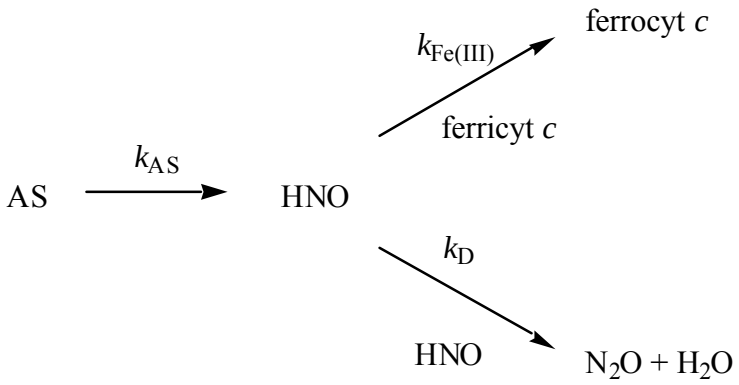

at the point of 50% product formation, the rates of each pathway are identical

$$k_{cytc}[\text{ferricyt c}][HNO] = 2k_{dimerization}[HNO]^2 \quad [\mathbf{4}]$$

or more generally,

$$k_s[S] = 2k_D[HNO]. \quad [\mathbf{5}]$$

To solve for k_S, [HNO] must be known. Assuming a steady-state of HNO and a quadratic solution (see Section D for complete derivation)

$$k_s = (1/[S])(k_D k_{AS}[AS])^{1/2} \quad [\mathbf{6}]$$

From Fig.1*A*, where $[S]_{0.5}$ is ≈4 μM ferricyt *c*, [AS] = 5 μM, $k_D = 8 \times 10^6$ $M^{-1}{\cdot}s^{-1}$ and k_{AS} $= 3 \times 10^{-3}{\cdot}s^{-1}$ (measured under the experimental conditions utilized and in fair agreement with the literature value of 5×10^{-3} s^{-1}; ref. 3), the rate constant for HNO reaction with ferricyt *c* is calculated from Eq. **6** to be 8.7×10^4 $M^{-1}{\cdot}s^{-1}$. However, because the conditions of the experiment did not allow for excess AS and because the rate-limiting step is decomposition of AS, the concentration of AS at 50% product should be half the original concentration. Using $[AS]_{0.5} = 2.5$ μM results in $k_S = 6.1 \times 10^4$ s^{-1}, which may not be a significant deviation.

Alternatively, from Fig. 1*B*, where 100 μM ferricyt *c* was exposed to varied AS resulting in $[AS]_{0.5} = 50$ μM, k_S is estimated to be 1.1×10^4 $M^{-1}{\cdot}s^{-1}$. Again, because neither reactant was in large excess, $[\text{ferricyt } c]_{0.5} = [\text{ferricyt } c]_{initial} - [P]_{0.5}$ or 100 μM – 25 μM = 75 μM. In this case, k_S is estimated to be 1.5×10^4 $M^{-1}{\cdot}s^{-1}$, again resulting in only a small deviation from the value calculated by using $[S]_{initial}$. The most significant difference arises when comparing each set of k_S values from Fig. 1 *A* and *B*; the difference in k_S calculated from the initial values is 8-fold, whereas the other set varies by only 4-fold. We used an average of all four values, 4×10^4 $M^{-1}{\cdot}s^{-1}$, in the remainder of the analysis.

Liochev and Fridovich (9) calculated that HNO reacts with ferricyt *c* with a rate constant of 3×10^5 $M^{-1}{\cdot}s^{-1}$ at 23°C. However, this was based on the dimerization rate constant of 4 $\times 10^9$ $M^{-1}{\cdot}s^{-1}$ (10). Using the revised rate constant this value decreases to 2×10^4 $M^{-1}{\cdot}s^{-1}$, which is in excellent agreement to our values considering the differences in temperature and the assumptions used in each estimation.

From Fig. 2*A*, where $[O_2] = 180$ μM and $[AS]_{0.5} = 11$ μM, the rate constant for the reaction between O_2 and HNO is calculated from Eq. **9** to be 3×10^3 $M^{-1}{\cdot}s^{-1}$. Because the derived rate constant for reaction of HNO with O_2 is an order of magnitude lower that that for ferricyt *c*, the complete quenching of HNO-mediated ferricyt *c* reduction

observed in aerobic buffer is likely not strictly a function of kinetics, and secondary reactions may be significant.

From the rate constants derived for ferricyt c (4×10^4 $M^{-1}{\cdot}s^{-1}$) and O_2 (3×10^3 $M^{-1}{\cdot}s^{-1}$), the rates for the other biomolecules can now be calculated from Eq. **2**

$$[S]_{initial}/[Q]_{0.5} = k_{quenching}/k_{monitored\ reaction} \qquad [\mathbf{2}]$$

and the ratio of concentrations given in Table 2. For instance, the 25-fold ratio for ferricyt *c* and SOD leads to a rate constant for the reaction of CuZnSOD with HNO of 1×10^6 $M^{-1}{\cdot}s^{-1}$. A similar value (7×10^5 $M^{-1}{\cdot}s^{-1}$) is obtained from the 225-fold difference between O_2 and CuZnSOD concentrations. Thus, the two separate detection systems yielded comparable results, offering some validation of the assumptions made. Recalculation of the rate constant for this reaction as estimated by Liochev and Fridovich (9) using the new dimerization constant (12) gives 9×10^4 $M^{-1}{\cdot}s^{-1}$ at 23°C. This suggests that the reactivity of HNO differs by nearly an order of magnitude between 23 and 37°C.

From the 600-fold ratio of O_2 to GSH, the rate constant for the reaction of GSH with HNO is estimated to be 2×10^6 $M^{-1}{\cdot}s^{-1}$ (Table 3). Consideration must be given to the fact that the calculated $[Q]_{0.5}$ for GSH of 0.3 μM falls slightly below the range of GSH utilized (0.5-5 mM). Changing the $[Q]_{0.5}$ for GSH to 0.4 or 0.2 μM alters the estimated rate constant by <1-fold. Utilizing 2×10^6 $M^{-1}{\cdot}s^{-1}$ as the assumed value, the rate constants for metMb, oxyMb and HRP are derived to be 8×10^5 $M^{-1}{\cdot}s^{-1}$, 1×10^7 $M^{-1}{\cdot}s^{-1}$ and 2×10^6 $M^{-1}{\cdot}s^{-1}$, respectively (Table 3).

The derived rate constant for MnSOD is 7×10^5 $M^{-1}{\cdot}s^{-1}$, which is 1.5-fold lower than for CuZnSOD. This difference may in part be due to the fact that the CuZn isoform is a homodimer with two metal centers, whereas MnSOD contains a single metal center. Normalizing to metal content, the rate constant for CuZnSOD drops to 5×10^5 $M^{-1}{\cdot}s^{-1}$.

The stoichiometry of the reaction of oxyMb and HNO (Eq. **3**) may also cause the calculated rate constant for that reaction to deviate from the absolute value.

Certainly, the rate constants in Table 3 should be considered to be only predictive, with a degree of uncertainty that will be refined with direct measurements using rapid time-resolved techniques. However, within the approximations made, these values offer insight for the first time into the reactions of HNO that are kinetically viable in biological systems.

D. Derivation for the equation utilized to calculate the rate constant from 50% product formation when dimerization is the competing reaction.

$$\frac{[P]}{[N_2O]} = \frac{k_S[S][HNO]}{k_D[HNO]^2}$$

$$[P] + 2[N_2O] = [AS]_T$$

$$[N_2O] = 0.5([AS]_T - [P])$$

Substitute for [S] and cancel [HNO]

$$\frac{[P]}{0.5([AS]_T - [P])} = \frac{k_S[S]}{k_D[HNO]}$$

Take the reciprocal

$$\frac{[AS]_T - 1}{[P]} = \frac{2k_D[HNO]}{k_S[S]}$$

At 50% product formation

$$\frac{[AS]_T}{} = 2$$

[P]

and thus

$$1 = \frac{2k_D[HNO]}{k_S[S]}$$

or

$$k_S = \frac{2k_D[HNO]}{[S]}$$

At constant [S], the concentration of AS at $[AS]_T/[P] = 2$ was determined experimentally, and k_D is known from the literature. Thus to calculate k_s, we must equate [AS] to [HNO]. Assuming a steady-state for [HNO]

$$-d[HNO]/dt = -2k_D[HNO]^2 - k_S[S][HNO] + k_{AS}[AS] = 0$$

This is a quadratic equation

$$x = \frac{-b \pm (b^2 - 4ac)^{1/2}}{2a} \qquad a = -2k_D \qquad b = -k_S[S] \qquad c = k_{AS}[AS]$$

Thus,

$$[HNO] = \frac{k_S[S] + (k_S^2[S]^2 + 8k_Dk_{AS}[AS])^{1/2}}{-4k_D}$$

Placing this solution back into

$$k_s = \frac{2k_D[HNO]}{}$$

[S]

gives

$$k_s = \frac{2k_D}{[S]} * \frac{(k_S[S] + (k_S^2[S]^2 + 8k_Dk_{AS}[AS])^{1/2}}{-4k_D}$$

To simplify this equation:

$$-2[S]k_S = k_S[S] + (k_S^2[S]^2 + 8k_Dk_{AS}[AS])^{1/2}$$

$$-3[S]k_S = k_S^2[S]^2 + 8k_Dk_{AS}[AS])^{1/2}$$

$$9[S]^2k_S^2 = k_S^2[S]^2 + 8k_Dk_{AS}[AS]$$

$$8[S]^2k_S^2 = 8k_Dk_{AS}[AS]$$

$$k_S^2 = 8k_Dk_{AS}[AS]/8[S]^2$$

$$k_S^2 = k_Dk_{AS}[AS]/[S]^2$$

and finally,

$$k_S = \frac{1}{[S].} * (k_Dk_{AS}[AS])^{1/2}$$

1. Wink, D. A., Feelisch, M., Fukuto, J., Chistodoulou, D., Jourd'heuil, D., Grisham, M. B., Vodovotz, Y., Cook, J. A., Krishna, M., DeGraff, W. G., *et al.* (1998) *Arch. Biochem. Biophys.* **351,** 66–74.

2. Miranda, K. M., Espey, M. G., Yamada, K., Krishna, M., Ludwick, N., Kim, S., Jourd'heuil, D., Grisham, M. B., Feelisch, M., Fukuto, J. M., *et al.* (2001) *J. Biol. Chem.* **276,** 1720–1727.

3. Maragos, C. M., Morley, D., Wink, D. A., Dunams, T. M., Saavedra, J. E., Hoffman, A., Bove, A. A., Isaac, L., Hrabie, J. A. & Keefer, L. K. (1991) *J. Med. Chem.* **34,** 3242–3247.

4. Paolocci, N., Saavedra, W. F., Miranda, K. M., Martignani, C., Isoda, T., Hare, J. M., Espey, M. G., Fukuto, J. M., Feelisch, M., Wink, D. A., *et al.* (2001) *Proc. Natl. Acad. Sci. USA.* **98,** 10463–10468.

5. Senzaki, H., Isoda, T., Paolocci, N., Ekelund, U., Hare, J. M. & Kass, D. A. *Circulation* **101,** 1040–1048.

6. Onuoha, G. N., Nugent, A. M., Hunter, S. J., Alpar, E. K., McEneaney, D. J., Campbell, N. P., Shaw, C., Buchanan, K. D. & Nicholls, D. P. (2000) *Eur. J. Clin. Invest.* **30,** 570–577.

7. Antonini, E. & Brunori, M. (1971) *Hemoglobin and Myoglobin in Their Reactions with Ligands* (North Holland, Amsterdam).

8. Mauk, M. R. & Girotti, A. (1974) *Biochemistry* **13,** 1757–1763.

9. Liochev, S. I. & Fridovich, I. (2002) *Arch. Biochem. Biophys.* **402,** 166–171.

10. Bazylinski, D. A. & Hollocher, T. C. (1985) *Inorg. Chem.* **24,** 4285–4288.

11. Gratzel, M., Taniguchi, S. & Henglein, A. (1970) *Ber. Bunsenges. Phys.* **74,** 1003–1010.

12. Shafirovich, V. & Lymar, S. V. (2002) *Proc. Natl. Acad. Sci. USA* **99,** 7340–7345.